

# Structural deformations and mechanical properties of Si<sub>2</sub>BN under uniaxial and uniform biaxial strain in comparison with graphene: an ab-initio study (Electronic Supplementary Information)

Zacharias G. Fthenakis<sup>1,2</sup> and Madhu Menon<sup>3</sup>

<sup>1</sup>*Department of Physics, University of South Florida, Tampa, Florida, 33620, USA*

<sup>2</sup>*Institute of Electronic Structure and Laser, FORTH, P.O. Box 1527, 71110 Heraklio, Crete, Greece*

<sup>3</sup>*Department of Physics and Astronomy, University of Kentucky, Lexington, Kentucky 40506, USA*

**Abstract of the main manuscript:** Si<sub>2</sub>BN has been recently predicted theoretically as a new entirely planar 2-dimensional material with a honeycomb-like structure, (like graphene), which is stable even at  $T > 1000$  K. In the present work we study the structural deformations and mechanical properties of Si<sub>2</sub>BN and graphene under both uniaxial (along the direction of the arm chair and zig-zag chains) and uniform biaxial tensile strain till the fracture limit and we compare those properties of the two structures with each other. According to our findings, in the Si<sub>2</sub>BN structure, Si-Si and Si-B bonds are weaker than B-N and Si-N bonds, respectively, contrary to graphene bonds, which all have the same strength. In particular, B-N bond lengths of Si<sub>2</sub>BN remain almost unchanged under the strain conditions we studied, not exceeding  $\approx 6\%$  of their initial length. Si<sub>2</sub>BN was found to be anisotropic, exhibiting large Young's and biaxial modulus values of the order of 1/3 and 2/5 of that of graphene, respectively. The different bond strengths in Si<sub>2</sub>BN explains its anisotropy and makes it behave very differently under strain when compared to graphene.

PACS numbers:

## I. INSTABILITY OF Si<sub>2</sub>BN FOR UNIFORM BIAxIAL STRAIN BEYOND $\varepsilon = 0.12$

According to our findings, the Si<sub>2</sub>BN structure becomes unstable if the uniform biaxial strain increases from  $\varepsilon = 0.12$  to  $\varepsilon = 0.13$  and any further increase in strain causes the breaking of the Si-Si bonds along a zig-zag chain leading to the formation of Si<sub>2</sub>BN ribbons, rather than having elongated (due to the strain) Si-Si bonds. Interestingly, however, the optimized structures obtained for  $\varepsilon = 0.12$  and  $0.13$  (shown in the left and the center of Fig. 1, respectively), did not initially favor the ribbon formation and thus concealing the evidence of instability for  $\varepsilon > 0.13$ . In particular, the energy as a function of the conjugate gradient steps for the optimization under  $\varepsilon = 0.13$  is shown with the black line in Fig. 1. However, distorting that optimized structure by shifting in the arm chair direction the topmost zig-zag chain of the unit cell by  $+\delta$ , the second one by  $+2\delta$  and the third one by  $+3\delta$ , where  $\delta = 0.002$  in fractional coordinates, and optimizing the structure again, the structure finds a lower energy minimum corresponding to the structure shown in right side of Fig. 1, where the breaking of the Si-Si bonds and the ribbon formation is evident. As we can see, between approximately the 10th and the 40th conjugate gradient step, the structure tended to reach the minimum that was previously found. However, optimization moved the structure past that minimum and into a even lower one. It is worth noting that along the conjugate gradient path that was followed after the 40th step no barrier was found indicating that there exists at least one path in the potential energy surface connecting the previous and the new minimum found. This lack of the existence of an energy barrier is proof that the previously found energy minimum is not a true minimum and, therefore, the structure corresponding to it is unstable.

In contrast to these results for  $\varepsilon = 0.13$ , the optimization of the similarly distorted structure for  $\varepsilon = 0.12$  led to the same energy minimum as the one already found, which implies that either the ribbon formation is not favored under those strain conditions, or there is an energy barrier that stabilizes the initially obtained optimum structure. The energy along the optimization path for the distorted structure for  $\varepsilon = 0.12$  is shown with the green line in Fig. 1.

## II. FITTING DETAILS FOR THE YOUNG'S MODULUS AND POISSON'S RATIO

To estimate the Young's modulus  $E$  for strain along either  $e_{zz}$  or  $e_{ac}$  directions, we fit a quadratic form to the points  $(\varepsilon, \sigma)$ , as well as a linear and a quadratic form to the points  $(\varepsilon, \sigma/\varepsilon)$ , where  $\varepsilon$  and  $\sigma$  are the strain and the stress, respectively, along the same direction ( $e_{zz}$  or  $e_{ac}$ ), for  $-0.05 \leq \varepsilon \leq 0.05$ .

To estimate the Poisson's ratio  $\nu$  along the same strain directions, we fit a quadratic form to the points  $(\varepsilon, -\varepsilon_{\perp}/\varepsilon)$  for  $-0.05 \leq \varepsilon \leq 0.05$ .

- For Si<sub>2</sub>BN

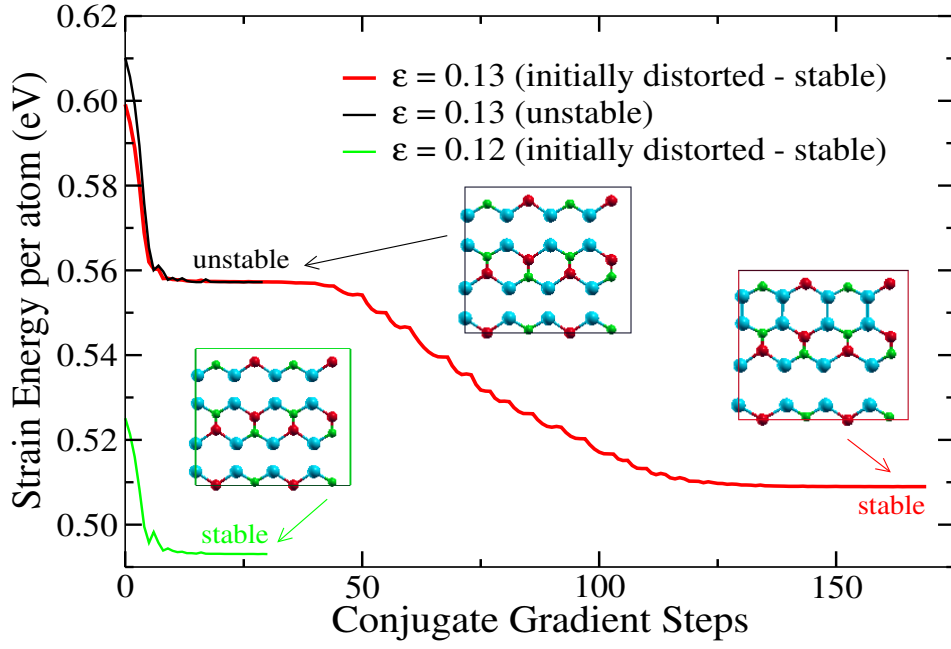


FIG. 1: (Color online). Strain energy per atom vs conjugate gradient optimization steps for distorted  $\text{Si}_2\text{BN}$  structure under strain  $\varepsilon = 0.12$  (green) and  $\varepsilon = 0.13$  (red), as well as non-distorted structure for  $\varepsilon = 0.13$  (see text for details).

– For Young's modulus along  $e_{zz}$  direction

$$\sigma = 0.002193 + 328.33\varepsilon - 614.18\varepsilon^2 \quad (\text{quadratic}), \quad E = 328 \text{ GPa} \quad (1)$$

$$E = \sigma/\varepsilon = 329.46 - 612.01\varepsilon \quad (\text{linear}), \quad E = 329 \text{ GPa} \quad (2)$$

$$E = \sigma/\varepsilon = 331.29 - 611.96\varepsilon - 1665\varepsilon^2 \quad (\text{quadratic}), \quad E = 331 \text{ GPa} \quad (3)$$

We adopt the value  $E = 330 \pm 2$  GPa.

– For Young's modulus along  $e_{ac}$  direction

$$\sigma = 0.0053729 + 374.16\varepsilon - 562.68\varepsilon_y \quad (\text{quadratic}), \quad E = 374 \text{ GPa} \quad (4)$$

$$E = \sigma/\varepsilon = 375.86 - 557.31\varepsilon \quad (\text{linear}), \quad E = 376 \text{ GPa} \quad (5)$$

$$E = \sigma/\varepsilon = 378.61 - 557.31\varepsilon - 2497.8\varepsilon^2 \quad (\text{quadratic}), \quad E = 379 \text{ GPa} \quad (6)$$

We adopt the value  $E = 376 \pm 3$  GPa

– For Poisson's Ratio along  $e_{zz}$  direction

$$\nu = -\varepsilon_{\perp}/\varepsilon = 0.30317 - 0.38775\varepsilon - 2.1073\varepsilon^2 \quad (\text{quadratic}), \quad \nu = 0.303 \quad (7)$$

– For Poisson's Ratio along  $e_{ac}$  direction

$$\nu = -\varepsilon_{\perp}/\varepsilon = 0.34506 - 0.82479\varepsilon + 0.54055\varepsilon^2 \quad (\text{quadratic}), \quad \nu = 0.345 \quad (8)$$

• For graphene

– For Young's modulus along  $e_{zz}$  direction

$$\sigma = -0.0048979 + 964.19\varepsilon - 2379.3\varepsilon^2 \quad (\text{quadratic}), \quad E = 964 \text{ GPa} \quad (9)$$

$$E = \sigma/\varepsilon = 964.20 - 2384.4\varepsilon \quad (\text{linear}), \quad E = 964 \text{ GPa} \quad (10)$$

$$E = \sigma/\varepsilon = 964.23 - 2384.2\varepsilon + 25.043\varepsilon^2 \quad (\text{quadratic}), \quad E = 964 \text{ GPa} \quad (11)$$

Therefore,  $E = 964 \text{ GPa}$ .

– For Young's modulus along  $e_{ac}$  direction

$$\sigma = -0.0078108 + 960.84\varepsilon - 1983.1\varepsilon^2 \quad (\text{quadratic}), \quad E = 961 \text{ GPa} \quad (12)$$

$$E = \sigma/\varepsilon = 963.39 - 1990.9\varepsilon \quad (\text{linear}), \quad E = 963 \text{ GPa} \quad (13)$$

$$E = \sigma/\varepsilon = 967.50 - 1990.9\varepsilon - 3739.6\varepsilon^2 \quad (\text{quadratic}), \quad E = 968 \text{ GPa} \quad (14)$$

We adopt the value  $E = 964 \pm 4 \text{ GPa}$ .

– For Poisson's ratio for strain along  $e_{zz}$

$$\nu = -\varepsilon_{\perp}/\varepsilon = 0.19007 - 0.43003\varepsilon - 1.6275\varepsilon^2, \quad (\text{quadratic}), \quad \nu = 0.190 \quad (15)$$

– For Poisson's ratio for strain along  $e_{ac}$

$$\nu = -\varepsilon_{\perp}/\varepsilon = 0.18858 - 0.68131\varepsilon + 1.5506\varepsilon^2, \quad (\text{quadratic}), \quad \nu = 0.189 \quad (16)$$

### III. UNDERSTANDING THE DIFFERENT BEHAVIOR OF POISSON'S RATIO IN $Si_2BN$ FOR STRAIN ALONG $e_{ac}$ AND $e_{zz}$ DIRECTIONS

To understand these behaviors we have to bear in mind that the lengths  $a$  and  $b$  of the vectors  $\mathbf{a}$  and  $\mathbf{b}$ , respectively, under strain along either  $e_{ac}$  or  $e_{zz}$  directions, are

$$a = 4 (d_{Si-N} \sin(\phi_1/2) + d_{Si-B} \sin(\phi_2/2)) \quad (17)$$

and

$$b = 2 (d_{Si-Si} + d_{B-N} + d_{Si-N} \cos(\phi_1/2) + d_{Si-B} \cos(\phi_2/2)), \quad (18)$$

where  $d_{A-B}$  is the length of the bond between atoms  $A$  and  $B$ , and  $\phi_1$  and  $\phi_2$  are the angles Si-N-Si and Si-B-Si, respectively. Consequently, the Poisson's ratio for the two strain directions is

$$\begin{aligned} \nu_{ac} &= -\frac{\varepsilon_{\perp}}{\varepsilon} = -\frac{a - a_0}{a_0\varepsilon} \\ &= -\frac{4}{a_0\varepsilon} (d_{Si-N} \sin(\phi_1/2) + d_{Si-B} \sin(\phi_2/2) - d_{0,Si-N} \sin(\phi_{01}/2) - d_{0,Si-B} \sin(\phi_{02}/2)) \\ &= -\frac{4}{a_0} \left( d_{0,Si-N} \frac{\delta \sin(\phi_1/2)}{\varepsilon} + d_{0,Si-B} \frac{\delta \sin(\phi_2/2)}{\varepsilon} + \frac{\delta d_{Si-N}}{\varepsilon} \sin(\phi_1/2) + \frac{\delta d_{Si-B}}{\varepsilon} \sin(\phi_2/2) \right) \end{aligned} \quad (19)$$

and

$$\begin{aligned} \nu_{zz} &= -\frac{\varepsilon_{\perp}}{\varepsilon} = -\frac{b - b_0}{b_0\varepsilon} \\ &= -\frac{2}{b_0\varepsilon} (d_{Si-Si} + d_{B-N} + d_{Si-N} \cos(\phi_1/2) + d_{Si-B} \cos(\phi_2/2) \\ &\quad - d_{0,Si-Si} - d_{0,B-N} - d_{0,Si-N} \cos(\phi_{01}/2) - d_{0,Si-B} \cos(\phi_{02}/2)) \\ &= -\frac{2}{b_0} \left( \frac{\delta d_{Si-Si}}{\varepsilon} + \frac{\delta d_{B-N}}{\varepsilon} + d_{0,Si-N} \frac{\delta \cos(\phi_1/2)}{\varepsilon} \right. \\ &\quad \left. + d_{0,Si-B} \frac{\delta \cos(\phi_2/2)}{\varepsilon} + \frac{\delta d_{0,Si-N}}{\varepsilon} \cos(\phi_1/2) + \frac{\delta d_{0,Si-B}}{\varepsilon} \cos(\phi_2/2) \right), \end{aligned} \quad (20)$$

where  $a_0$ ,  $b_0$ ,  $d_{0,AB}$ ,  $\phi_{01}$  and  $\phi_{02}$  are the values of  $a$ ,  $b$ ,  $d_{AB}$ ,  $\phi_1$  and  $\phi_2$ , respectively, at zero strain, and  $\delta d_{A-B} = d_{A-B} - d_{0,A-B}$ ,  $\delta \cos(\phi_i/2) = \cos(\phi_i/2) - \cos(\phi_{0i}/2)$  and  $\delta \sin(\phi_i/2) = \sin(\phi_i/2) - \sin(\phi_{0i}/2)$ ,  $i = 1, 2$ . Therefore, the expression for  $\nu_{ac}$  has four terms, while the one for  $\nu_{zz}$  has six. Those terms correspond to specific contributions to the Poisson's ratio, and they are shown in Fig. 2.

It becomes clear from panel (a) of this figure that the second and third terms of the final expression of the above equation for  $\nu_{zz}$  (i.e the terms  $d_{0,Si-N}\delta \cos(\phi_1/2)/\varepsilon$  and  $d_{0,Si-B}\delta \cos(\phi_2/2)/\varepsilon$ ) are the terms providing the most important contributions to the Poisson's ratio for strain along  $e_{zz}$ . The rest of the terms are rather small and their cumulative contribution is more or less constant with a value approximately equal to -0.1. Thus, summing up the the third and fourth term and subtracting -0.1 from that sum, we take a curve very close to the curve of  $\nu_{zz}$ , as is shown with the light blue line in Fig. 2(a). This indicates that the behavior of  $\nu_{zz}$  as a function of the strain is mainly governed by the competition between these two terms, which represent the contributions from the bending of the angles Si-N-Si and Si-B-Si. The former increases as a function of strain, while the latter decreases at first and then increases with none of them showing a linear relation as a function of strain.

In turn, panel (b) of that figure shows the corresponding contributions to  $\nu_{ac}$  of the terms of the final expression of the above equation for  $\nu_{ac}$ . As seen in the figure, all terms rise almost linearly with strain, having as a result an almost linear decrease of  $\nu_{ac}$  as a function of strain. Again the main contributions come from the terms associated with the angle bending deformations (i.e. from the first ( $d_{0,Si-N}\delta \sin(\phi_1/2)/\varepsilon$ ) and the second  $d_{0,Si-B}\delta \sin(\phi_2/2)/\varepsilon$ ) terms of that expression. What we can also see from that figure, is that the curve of the second term is very similar to the curve of  $\nu_{ac}$ , which indicates that the rest of the terms are more or less canceled with each other.

#### IV. FITTING DETAILS FOR THE BIAxIAL ELASTIC MODULI $M_x$ AND $M_y$

To find the biaxial elastic moduli  $M_x$  and  $M_y$  we fit a second, third and fourth order polynomial to the points  $(\varepsilon, \sigma_x)$  and  $(\varepsilon, \sigma_y)$  for  $-0.05 \leq \varepsilon \leq 0.05$ . Second and third order polynomial fits were not as successful as the fourth order, which were finally selected to derive the biaxial elastic moduli values. The fitting functions found were the following:

- For graphene

$$\sigma = 1218.72\varepsilon - 6012.47\varepsilon^2 \quad (21)$$

$$\sigma = 1188\varepsilon - 6012.47\varepsilon^2 + 17255.1\varepsilon^3 \quad (22)$$

$$\sigma = 1188\varepsilon - 6463.36\varepsilon^2 + 17255.1\varepsilon^3 + 215170\varepsilon^4. \quad (23)$$

- For Si<sub>2</sub>BN

$$\sigma_{xx} = 484.092\varepsilon - 2078.19\varepsilon^2, \quad (24)$$

$$\sigma_{xx} = 502.334\varepsilon - 2078.19\varepsilon^2 - 10248.2\varepsilon^3, \quad (25)$$

$$\sigma_{xx} = 502.334\varepsilon - 2600.26\varepsilon^2 - 10248.2\varepsilon^3 + 249136\varepsilon^4, \quad (26)$$

and

$$\sigma_{xx} = 542.699\varepsilon - 2419.29\varepsilon^2, \quad (27)$$

$$\sigma_{xx} = 557.544\varepsilon - 2419.29\varepsilon^2 - 8339.46\varepsilon^3, \quad (28)$$

$$\sigma_{xx} = 557.544\varepsilon - 2930.58\varepsilon^2 - 8339.46\varepsilon^3 + 243991\varepsilon^4. \quad (29)$$

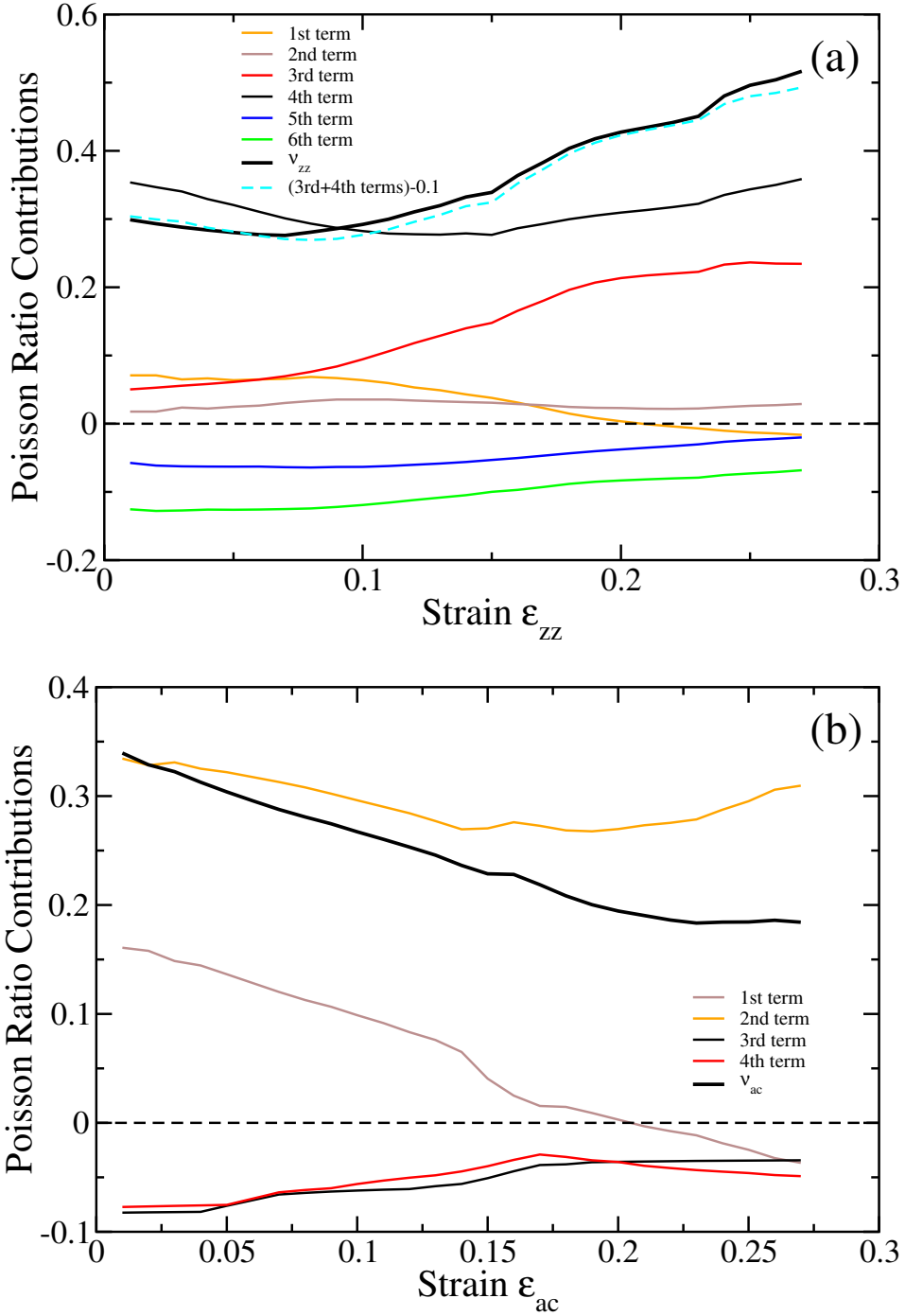


FIG. 2: (Color online). Contributions to the Poisson's ratio from the terms of Eqs. 19 and 20 of ESI for  $\text{Si}_2\text{BN}$  under strain along (a)  $e_{ac}$  and (b)  $e_{ac}$  directions, respectively.

## V. DERIVATION OF EQUATIONS FOR BIAxIAL MODULI FROM YOUNG'S MODULUS AND POISSON'S RATIO

For uniaxial strain  $\epsilon_x$  along x-direction, the Young's modulus is  $E_x = \sigma_{xx}/\epsilon_x$  and the Poisson's ratio is  $\nu_{xy} = -\epsilon_y/\epsilon_x$ . Therefore,  $\epsilon_x = \sigma_{xx}/E_x$  and  $\epsilon_y = -\nu_{xy}\sigma_{xx}/E_x$ .

Accordingly, for uniaxial strain  $\epsilon_y$  along y-direction, the Young's modulus is  $E_y = \sigma_{yy}/\epsilon_y$  and the Poisson's ratio is  $\nu_{yx} = -\epsilon_x/\epsilon_y$ . Therefore,  $\epsilon_y = \sigma_{yy}/E_y$  and  $\epsilon_x = -\nu_{yx}\sigma_{yy}/E_y$ .

If strain is applied simultaneously in both directions, the strains  $\epsilon_x$  and  $\epsilon_y$  obtained for the two uniaxial strain

directions will be combined, and the strains along  $x$  and  $y$  directions will be

$$\varepsilon_x = \frac{\sigma_{xx}}{E_x} - \nu_{yx} \frac{\sigma_{yy}}{E_y} \quad \text{and} \quad \varepsilon_y = -\nu_{xy} \frac{\sigma_{xx}}{E_x} + \frac{\sigma_{yy}}{E_y}, \quad (30)$$

which leads to

$$\sigma_{xx} = E_x \frac{\varepsilon_x + \nu_{yx} \varepsilon_y}{1 - \nu_{xy} \nu_{yx}} \quad \text{and} \quad \sigma_{yy} = E_y \frac{\varepsilon_y + \nu_{xy} \varepsilon_x}{1 - \nu_{yx} \nu_{xy}}. \quad (31)$$

For uniform biaxial strain,  $\varepsilon_x = \varepsilon_y = \varepsilon$  and consequently

$$\sigma_{xx} = E_x \frac{1 + \nu_{yx}}{1 - \nu_{xy} \nu_{yx}} \varepsilon \quad \text{and} \quad \sigma_{yy} = E_y \frac{1 + \nu_{xy}}{1 - \nu_{yx} \nu_{xy}} \varepsilon. \quad (32)$$

Thus, the elastic moduli  $M_x = \sigma_{xx}/\varepsilon$  and  $M_y = \sigma_{yy}/\varepsilon$  become

$$M_x = E_x \frac{1 + \nu_{yx}}{1 - \nu_{xy} \nu_{yx}} \quad \text{and} \quad M_y = E_y \frac{1 + \nu_{xy}}{1 - \nu_{yx} \nu_{xy}}. \quad (33)$$

In particular, for an isotropic material, like graphene, where  $E_x = E_y = E$  and  $\nu_{xy} = \nu_{yx} = \nu$ , the above relations yield

$$M = M_x = M_y = \frac{E}{1 + \nu} \quad (34)$$